*Letter*

# A Predictive Analysis of Differential Attenuation on Adjacent Satellite Paths Including Rain Height Effects

JOHN D. KANELLOPOULOS, DIONYSIOS MARGETIS
Division of Electroscience Department of Electrical and Computer Engineering
National Technical University of Athens
9 Iroon Polytechniou Street, Zografou, GR-15773 Athens - Greece

**Abstract.** Interference between adjacent Earth-space paths can be caused by propagation effects due to differential rain attenuation. In the present paper, a modification of an existing method to predict the rain differential attenuation statistics is proposed. The modified method takes into account a more complicated but realistic model for the description of the rain height. The present results are compared with the available simulation data for the differential attenuation over pairs of paths in the Montreal area. The difference between the existing predictive results and the deduced ones after use of the modified procedure, for various geographic latitudes and climatic zones, is also examined.

## 1. INTRODUCTION

An interesting problem in the design of a satellite communication system can arise when two satellites operating at the same frequency are separated from one another by a small angle $\theta$ as viewed from an Earth station (Fig. 1). Because of the spatial inhomogeneity in the precipitation, periods of time can exist in which the wanted signal may suffer a large attenuation, due to heavy rain while, at the same time, the unwanted signal may experience a much lower attenuation in weaker rain. When this difference in attenuation becomes sufficiently large, then the signal from the adjacent satellite can cause interference. The analysis of the above interference, due to differential rain attenuation between adjacent paths, leads to the consideration of the joint effects of rain attenuation $A_c$ of the intended signal and the rain attenuation $A_I$ of the potential interfering signal. For interference calculations, the conditional distribution of $\Delta A = A_c - A_I$ under the condition 0.5 dB $< A_c < M$, where $M$ is the maximum allowed attenuation of the wanted signal, should be used. In this sense, Rogers et al [1] have first proposed an empirical model for the differential rain attenuation $\Delta A$ at the 1% conditional probability level, valid for the frequency range from 11 to 30 GHz, for elevations from 5° to 30°, angular separations from 2° to 9°, and system margins from 2 to 10 dB. The above model, although simple is provisional and must be used with caution [2]. Further, Kanellopoulos and Houdzoumis [3] suggested a predictive method for the differential attenuation statistics based on a model of convective raincells and the lognormal model for the point rainfall rate statistics. More recently, a revised version of this predictive technique has been presented [4] by considering different elevation angles for the two slant paths. It is worthwhile to notice here, that other problems of this type arising in the satellite communication analysis and regarding the differential attenuation interference from an adjacent terrestrial system, have also been handled by employing the latter technique [5, 6].

The predictive procedure under discussion, is quite flexible and is oriented to be applicable to any location of the world where the above assumptions are satisfied. A fundamental consideration of the predictive methodology is also concerned with the estimation of the rain height. For this reason, a constant rain height equal to the height of the 0°C isotherm, dependent upon the latitude of the location [7] has been used throughout the analysis there.

Towards this direction, it is our intention to consider here for our interference prediction problem, a more realistic model for the effective rain height suggested by Stutzman and Dishman [8], consisting of using the 0°C isotherm height for low rainrates and adding a rainrate dependent term to the 0°C isotherm height for higher rainrates. This is consistent with the radar reflectivity profiles given by Goldhirsh and Katz [9], where it is shown that the rain height is equal to the height of the 0°C isotherm for low rainrates. As rainrate increases, the rain height indicated by the reflectivity profiles also increases. This increase is due to the structure of convective raincells in

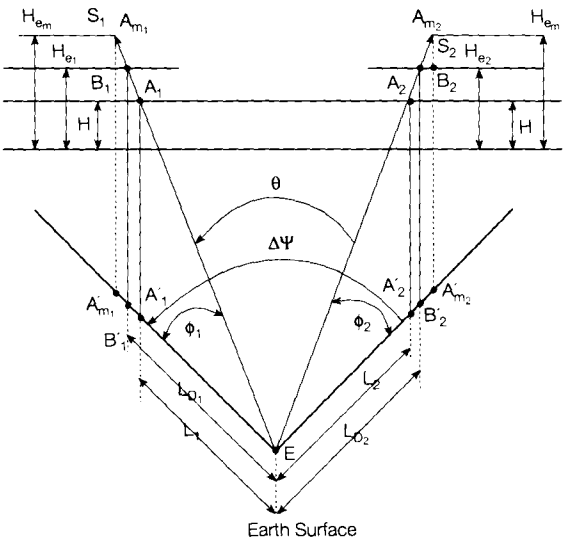


**Fig. 1** - Configuration of the problem.

which liquid water may be carried well above the 0°C isotherm level by updrafts. The rain height model under discussion has already been employed [8] for the development of an effective technique for the estimation of the rain induced attenuation along earth-space paths with very good performance in the important region of low percentages of time, compared to experimental data from all over the world. Further, the same novel assumptions for the effective rain height have been used for the analysis of the outage performance of a multiple site diversity Earth-space system [10]. It is worthwhile to notice here that another consideration for the rain height model has also recently been adopted. Following this consideration, the rain height was assumed to be a random variable uncorrelated to rainrate, whose median annual value depends on rainrate. This model was applied to a similar problem, that is the prediction of the interference due to hydrometeor scatter on satellite communication links [11]. However, Olsen et al [12] denote that neither the fixed rain height model nor that of random rain height uncorrelated to rainrate seem universally realistic physically.

In the present paper, the modified analysis for the prediction of differential rain attenuation is developed, by taking into account the model suggested by Stutzman and Dishman [8] for the rain height. Numerical results taken from the proposed procedure are compared with the only existing set of simulated data from the Montreal area. In addition, the difference between the existing predictive results and the deduced ones due to employment of the novel assumptions for the rain height, for various geographic latitudes and climatic zones, is finally examined.

## 2. The Analysis

The analytical configuration of the problem is shown in Fig. 1. The two satellites have different elevation angles $\varphi_1$, $\varphi_2$ and they are separated from one another by a small angle $\theta$ as viewed from the Earth station. $\Delta\Psi$ is also the projected differential angle between the slant paths under consideration. The description of the parameters $H_{e_1}$, $H_{e_2}$ and $H$ is given in subsection 2.1. The main point of the interference analysis is the evaluation of the differential attenuation statistics given by

$$P(\Delta A \geq r/0.5 \leq A_c \leq M) = \frac{P(\Delta A \geq r, 0.5 \leq A_c \leq M)}{P(0.5 \leq A_c \leq M)} \tag{1}$$

where $A_c$ is the attenuation of the desired signal, $A_I$ the attenuation of the potential interfering signal, $r$ the exceeded differential attenuation level and $M$ the system margin available for rain attenuation.

### 2.1. *General considerations*

The following considerations which are required for the analysis are taken into account.

1) Crane's simplified consideration for the vertical variation of the rainfall structure is first employed [7]. This leads to the assumption of uniform rain structure from the ground up to an effective rain height $H_e$. As mentioned previously, we will consider here the model proposed by Stutzman and Dishman [8] for the determination of the rain height $H_e$. According to this consideration, the latter parameter is dependent not only on $\Lambda$ (geographic latitude of the specific location) but also upon the value of the corresponding point rainfall rate $R$. As a result, we have

$$\left.\begin{aligned} H_e &= H && \text{for} \quad R \leq 10 \text{ mm/h} \\ H_e &= H + \log\left(\frac{R}{10}\right) && \text{for} \quad R > 10 \text{ mm/h} \end{aligned}\right\} \tag{2}$$

where

$$\left.\begin{aligned} H &= 4.8 \text{ km} && |\Lambda| \leq 30^\circ \\ H &= \left(7.8 - 0.1.\frac{|\Lambda|}{\text{deg}}\right) \text{km} && |\Lambda| > 30^\circ \end{aligned}\right\} \tag{3}$$

It should be noted here that another expression for the mean seasonal value $H$ as a function of $\Lambda$, is also valid [13], but the results are the same. Let us now consider the configuration of the satellite path $i$ ($i$ =1, 2) (Fig. 1). We define now two points characteristic for the further analysis: $A_i$ and $A_{m_i}$ which are the section points of the slant path $ES_i$ and the levels $H$ and $H_{e_m}$, respectively. The effective rain height $H_{e_m}$ is evaluated by means of eq. (2) and is related to some maximum observed rainfall rate (say 150 – 200 mm/h). The rain height $H_e$ varies generally with rain rate and as a direct result the effective slant path length is also a function of the rainrates referring to all points inside the part $A_i' A_{m_i}'$ (Fig. 1) for rainrates between 10 and $R_m$ mm/h. The application of

the above consideration leads to cumbersome and very complicated calculations but this situation can be avoided by assuming the homogeneity of the rainfall medium inside the part $A_i' A_{m_i}'$. Following this assumption the effective lengths of the satellite paths are given by

$$L_{S_i} = \frac{H_{e_i} - H_o}{\sin \varphi_i}, \quad \varphi_i \geq 10^\circ \qquad (i = 1,2) \tag{4}$$

where the level $H_{e_i}$ depends upon the point rainrate $R_{A_i}$ with respect to $A_i$. This assumption can be shown to be valid for elevation angles greater than about 10°, leading to projected straightline parts $A_i' A_{m_i}'$ of the order of a few kilometers. Moreover, $H_o$ is the average height above sea level of the Earth station.

According to the assumption of uniform vertical rain structure, the single and joint exceedance probabilities (eq. (1)) can be obtained as

$$P(0.5 \leq A_c \leq M) = P(0.5 \cos \varphi_1 \leq A_c' \leq M \cos \varphi_1) \tag{5}$$

and

$$P\left[\Delta A \geq r,\ 0.5 \leq A_c \leq M\right] = P\left[ A_I' \leq A_c' \frac{\cos \varphi_2}{\cos \varphi_1} - r \cos \varphi_2, 0.5 \cos \varphi_1 \leq A_c' \leq M \cos \varphi_1 \right] \tag{6}$$

where

$$\Delta A = A_c - A_I \tag{7}$$

and $A_c'$, $A_I'$ are the attenuations referring to hypothetical terrestrial links which are the projections of the slant paths affected by the rain medium, with path lengths

$$L_{D_i} = L_{S_i} \cos \varphi_i \quad (i = 1, 2) \tag{8}$$

2) All the other assumptions are similar to those employed for the analysis of the previous [3, 4] methodology using the constant rain height model and they are briefly presented here.

The lognormal form for the unconditional (including non raining time) point rainfall rate $R$ and attenuation $A$ distributions is first adopted.

Next, the specific rain attenuation (in dB/km) is considered to be given by the following expression

$$A_0 = a R^b \tag{9}$$

where $R$ is the rainrate and the constants a and $b$ depend upon frequency, incident polarization, temperature and raindrop size distribution.

The convective raincell model proposed by Lin [14] is finally employed, for the description of the horizontal variation of the rainfall medium. According to this model, the spatial correlation coefficient $\rho_0$ (d) of attenuation gradient $A_0$ between two points of the rain medium is given by

$$\rho_0 = \frac{G}{\sqrt{G^2 + d^2}} \tag{10}$$

where $G$ is a characteristic parameter depending on the spatial structure of the rainfall medium for the specific location.

### 2.2. *Evaluation of the differential attenuation probability*

As mentioned previously, the difference of the present contribution with respect to earlier work [3, 4] is that this paper attempts at taking into account a more realistic description of the rain height during rain conditions [8]. Since this appears to be the only difference, the expressions relating the probabilities (5) and (6) to the lognormal statistical parameters $A_{m_1}$, $S_{\alpha_1}$ and $A_{m_2}$, $S_{\alpha_2}$ of the attenuations corresponding to wanted and interfering signals as well as the logarithmic correlation coefficient $\rho_{n_{12}}$ between them, remain the same. A reference to [3, 4] is considered sufficient. On the other hand, the influence of the novel rain height considerations upon the calculation of the above statistical parameters is very crucial. The evaluation of the $A_{m_1}$, $S_{\alpha_1}$ and $A_{m_2}$, $S_{\alpha_2}$ in this case can proceed by expressing these parameters as [15]

$$\left.\begin{aligned} S_{\alpha_i}^2 &= \ln\left[\frac{\sigma_{A_i}^2}{\mu_{A_i}^2} + 1\right] \\ A_{m_i} &= \frac{\mu_{A_i}^2}{\sqrt{\sigma_{A_i}^2 + \mu_{A_i}^2}} \end{aligned}\right\} \quad (i = 1,2) \tag{11}$$

in terms of the mean values ($\mu_{A_i}$) and standard deviations ($\sigma_{A_i}$) of the variables $A_c'$ and $A_I'$, respectively. Following a cumbersome but straightforward analysis the $\mu_{A_i}$ and $\sigma_{A_i}$ have been expressed by means of the lognormal statistical parameters $R_m$ (median value) and $S_r$ (standard deviation) of the point rainfall distribution, the constants a and $b$ of the specific attenuation ($A_0 = aR^b$) and the characteristic distance $G$ (section 2.1), as

$$\mu_{A_i} = a m_b L_i + \frac{a m_b}{2 \tan \varphi_i} \log e \cdot \left\{ \left[ \ln\left(\frac{R_m}{10}\right) + b S_r^2 \right] \operatorname{erfc}(t_o) + \sqrt{\frac{2}{\pi}}\, S_r\, e^{-t_o^2} \right\} \tag{12}$$

$(i = 1, 2)$

where

$$L_i = \frac{H - H_o}{\tan \varphi_i} \tag{13}$$

$$m_b = R_m^b \exp\left(\frac{b^2 S_r^2}{2}\right) \tag{14}$$

$$t_o = \frac{u_o - b S_r}{\sqrt{2}} \tag{15}$$

$$u_o = \frac{\ell n(10/R_m)}{S_r} \tag{16}$$

and

$$\left.\begin{aligned}\sigma_{A_1}^2 &= E\left[A_c'^2\right] - \mu_{A_1}^2 \\ \sigma_{A_2}^2 &= E\left[A_I'^2\right] - \mu_{A_2}^2\end{aligned}\right\} \tag{17}$$

where

$$E\left[A_c'^2\right] = I_{11} + 2I_{1d} + I_{dd_1} \tag{18}$$

$$E\left[A_I'^2\right] = I_{22} + 2I_{2d} + I_{dd_2} \tag{19}$$

Further,

$$I_{ii} = a^2\,\sigma_b^2\,H_{ii} + a^2\,m_b^2\,L_i \tag{20}$$

$$\sigma_b^2 = m_{2b} - m_b^2 \tag{21}$$

$$H_{ii} = 2\,L_i\,G\sin h^{-1}\left(\frac{L_i}{G}\right) + 2G^2\left\{1 - \left[\left(\frac{L_i}{G}\right)^2 + 1\right]^{1/2}\right\} \tag{22}$$

and the analytical expressions for $I_{id}$ and $I_{ddi}$ can be found in [10], where the same novel assumptions for the effective rain height have been used for the analysis of the improvement due to the employment of the multiple site diversity technique.

Moreover, the calculation of the $\rho_{n_{12}}$ which is the logarithmic correlation coefficient between the attenuations $A_c'$ and $A_I'$ follows quite similar steps. Generally, we have [4]

$$\rho_{n_{12}} = \frac{1}{S_{\alpha_1}\cdot S_{\alpha_2}}\,\ell n\left[1 + \rho_{12}\sqrt{\left(e^{S_{\alpha_1}^2} - 1\right)\left(e^{S_{\alpha_2}^2} - 1\right)}\right] \tag{23}$$

and the path correlation $\rho_{12}$ is expressed as

$$\rho_{12} = \frac{E\left(A_c'\,A_I'\right) - \mu_{A_1}\cdot\mu_{A_2}}{\sigma_{A_1}\cdot\sigma_{A_2}} \tag{24}$$

Following again a similar statistical analysis as before for the $\mu_{A_i}$ and $\sigma_{A_i}$, one gets

$$E\left(A_c'\,A_I'\right) = K_{12} + K_{1d} + K_{2d} + K_{dd} \tag{25}$$

where

$$K_{12} = a^2\,\sigma_b^2\,H_2 + a^2\,m_b^2\,L_1\,L_2 \tag{26}$$

and the analytical derivation of $H_2$ can be found elsewhere [4]. As far as the other terms of (25) are concerned, we have

$$K_{1d} = \frac{a^2\log e}{2\tan\varphi_2}\,m_b^2\;\ell\left(L_1, L_2, \Delta\Psi\right) \tag{27}$$

$$K_{2d} = \frac{a^2\log e}{2\tan\varphi_1}\,m_b^2\;\ell\left(L_2, L_1, \Delta\Psi\right) \tag{28}$$

$$K_{dd} = \frac{a^2\log^2 e}{2\tan\varphi_1\,\tan\varphi_2}\,R_m^{2b}\cdot \exp\left\{b^2\,S_r^2\left[1+\rho_n'\left(L_1, L_2, \Delta\Psi\right)\right]\right\}\left\{\xi_1\left[\operatorname{erf} c\left(S_o\right) - K\right] + \xi_2\,e^{-S_o^2}\operatorname{erf} c\left[S_o\sqrt{\frac{1-\rho_n'\left(L_1, L_2, \Delta\Psi\right)}{1+\rho_n'\left(L_1, L_2, \Delta\Psi\right)}}\right] + \xi_3\,e^{-2S_o^2/\left[1+\rho_n'\left(L_1, L_2, \Delta\Psi\right)\right]}\right\} \tag{29}$$

where

$$\rho_n'\left(L, z, \gamma\right) = \frac{1}{b^2\,S_r^2}\,\ell n\left[1 + \rho_o'\left(L, z, \gamma\right)\left(e^{b^2\,S_r^2} - 1\right)\right] \tag{30}$$

$$\rho_o'\left(L, z, \gamma\right) = \frac{G}{\sqrt{G^2 + L^2 + z^2 - 2\,z\,L\cos\gamma}} \tag{31}$$

and the analytical expressions for $\ell(L_1, L_2, \Delta\Psi)$, $\xi_1$, $\xi_2$, $\xi_3$, $S_o$ and $K$ can also be found in [10].

## 3. Numerical results and discussion

In this section, an application of the above analysis for the prediction of the differential attenuation probability, is presented. First, the proposed predictive procedure has been applied to the simulated data for the differential rain attenuation taken from Montreal [1]. More particularly, forty hours of observations of the three-dimensional radar reflectivity structure of rain in the Montreal area were used to simulate the attenuations occuring simultaneously over a multitude of earth-space propagation paths. It is worthwhile to notice here that the same data base was used in an earlier radar-radiometer comparison [16], which demonstrated that the attenuation statistics generated synthetically by integrating the measured radar reflectivity over earth-space propagation paths were in good agreement with independently measured attenuation statistics for the same paths. The compilation of statistics on differential attenuation on adjacent paths was succeeded by simulating a large number of pairs of paths for a variety of viewing directions, frequencies, elevation angles, angular separations, and taking values of attenuation occuring simultaneously over the paths computed at 5 min intervals. Further details concerning this matter are given in [1].

On the other hand, the implementation of the proposed procedure requires the knowledge of the parameters $H$, $H_o$, $a$, $b$, $G$, $R_m$ and $S_r$ with respect to the Montreal data under consideration. A list of appropriate numerical val-

Table 1 - *Parameters of the Montreal experiment*

| Parameter | Value | |
|---|---|---|
| $H$ | 3.2 km | |
| $H_o$ | 0.2 km | |
| $G$ | 0.75 km | |
| $R_m$ | 0.049 | |
| $S_r$ | 1.74194 | |
| $a$ | (15 GHz) 0.0295 | (30 GHz) 0.1581 |
| $b$ | 1.1418 | 1.0427 |

ues for these parameters is presented in Table 1. Some comments concerning the proper estimation of the above parameters are presented elsewhere [3].

In Figs. 2 - 4, the conditional probability has been drawn versus the variable $r$ in comparison with the simulated data, for various values of frequency $f$, elevation angles $\varphi$, angular separations $\theta$ and available margins $M$. In the same figures, the results taken from the existing procedure [3, 4] are also drawn. As can be seen, the comparison shows an improved situation in relation to the already existing ones.

In addition, the differential attenuation at the 1% conditional probability $\Delta A(1\%)$ is also examined. More particularly, $M$ (available margin in decibels) curves versus the angular separation $\theta$ (in degrees) are shown for $\Delta A(1\%)$ = 1 dB, $f$ = 15 GHz and $\varphi_1 = \varphi_2 = 10°, 20°$ (Figs. 5 and 6). As pointed out by Rogers et al [1], the reason for the

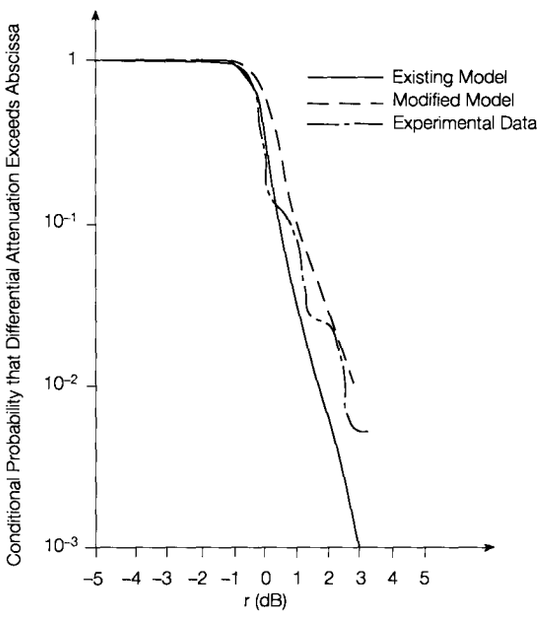


**Fig. 2** - The conditional probability $P$ ($\Delta A \geq r/0.5 \leq A_c \leq M$) versus the variable $r$, for $f$ = 15 GHz, $M$ = 5 dB, $\varphi_1 = \varphi_2 = 10°$, $\theta = 6°$ and Montreal area.

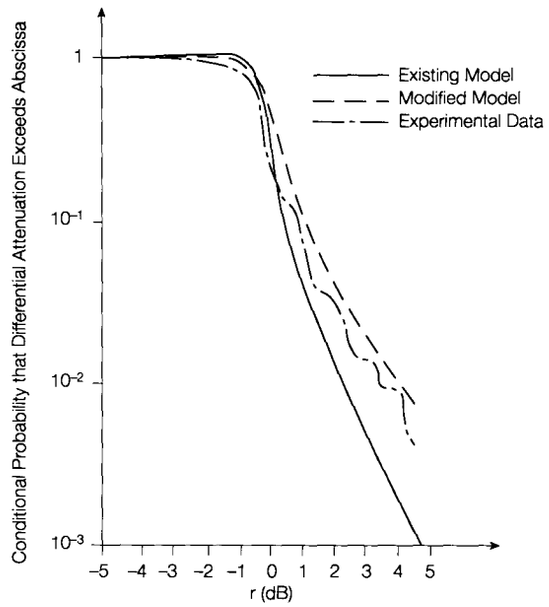


**Fig. 3** - The same as in Fig. 2 but for $M$ = 10 dB.

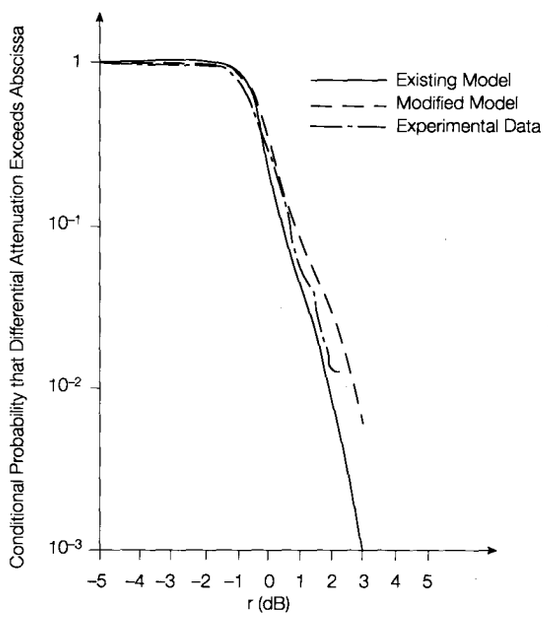


**Fig. 4** - The same as in Fig. 2 but for $f$ = 30 GHz, $M$ = 5 dB, $\varphi_1 = \varphi_2 = 10°$, $\theta = 6°$.

choise of these coordinates ($M$ and $\theta$) is that the angular separation and margin are the parameters over which the system designer probably has the most control. The same improved situation, with respect to the experimental data, is also quite obvious. All the above facts seem to justify the necessity for the development of the present method which takes into account more complicated but realistic considerations for the estimation of the rain height.

Further, similar curves ($M$ versus $\theta$) are examined for various locations (Japan, Florida and Denmark) in comparison with the existing predictive results (Figs. 7 - 9). In this case, experimental data are not available. As it is obvious, the deviation between the results taken from the present predictive technique and the already existing

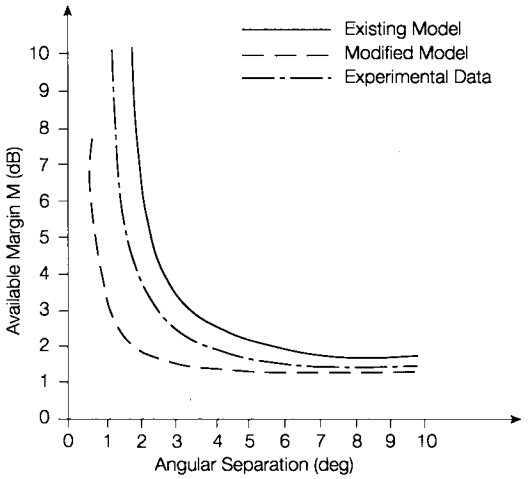


**Fig. 5** - Available margin $M$ (in dB) versus the angular separation $\theta$ (in degrees) for $f$ = 15 GHz, $\varphi_1 = \varphi_2 = 10°$, $\Delta A$ (1%) = 1 dB (Montreal area).

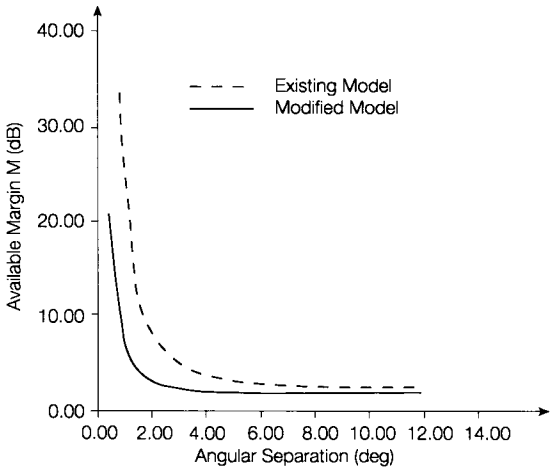


**Fig. 7** - Available margin $M$ (in dB) versus the angular separation $\theta$ (in degrees) in comparison with the existing predictive procedure: $f$ = 15 GHz, $\varphi_1 = \varphi_2 = 30°$, $\Delta A$ (1%) = 1dB (Florida area).

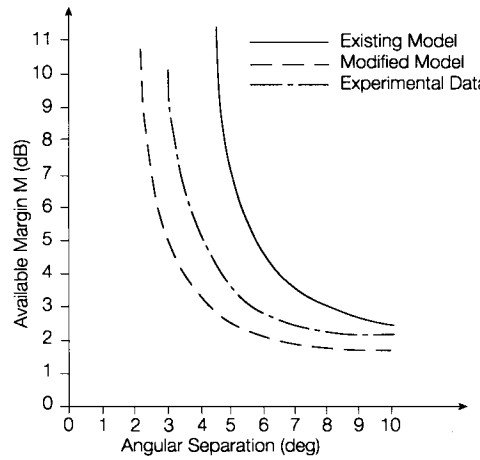


**Fig. 6** - The same as in Fig. 5 but for $\varphi_1 = \varphi_2 = 20°$.

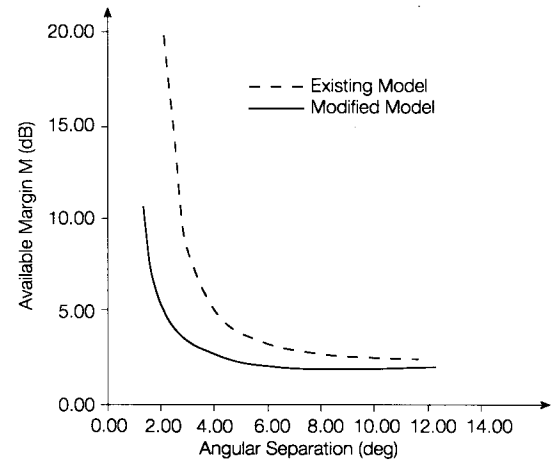


**Fig. 8** - The same as in Fig. 7 but for Japan area.

one is not quite evident for low absolute latitude locations even associated with high rainfall conditions such as the Florida area ($\Lambda = 28°$, Fig.7). On the other hand, there is a gradually increasing deviation in relation to the absolute latitude of the location and this is quite pronounced for latitudes greater than 50° even associated with low rainfall conditions such as the Denmark area ($F$ climatic zone, $\Lambda = 60°$, Fig.9).

Another set of curves which the system designer would like to see is the effective carrier -to- interference ratio ($C/I$) versus the angular separation ($\theta$) of the two satellites. Following basic satellite link considerations [17], the ($C/I$) ratio of an earth-space system interfered by an adjacent satellite, under clear-sky conditions, is given by

$$\left(\frac{C}{I}\right)_{c.s} = \mathrm{EIRP_s(dBW)} - \mathrm{EIRP_s'(dBW)} + G(\mathrm{dB}) - (32 - 25\log\theta) \quad (32)$$

where $\mathrm{EIRP_s}$ is the equivalent isotropic radiated power of interfered satellite $S_1$ in the direction of interfered earth station $E$. Moreover, $\mathrm{EIRP_s'}$ is the equivalent isotropic radiated power of interfering satellite $S_2$ in the direction of interfered earth station $E$ and $G$ is the on-axis received antenna gain of interfered earth station $E$. The last term of the eq. (32) specifies a sidelobe envelope level relative to the normalized peak gain (0 dB)

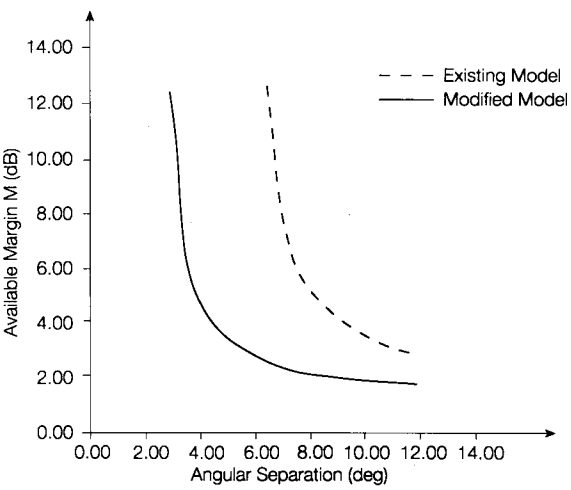


**Fig. 9** - The same as in Fig. 7 but for Denmark area ($F$ climatic zone).

according to the U.S. Federal Communications Commission [17]. The carrier -to- interference ratio under rain fading conditions is now expressed as

$$\left(\frac{C}{I}\right)=\left(\frac{C}{I}\right)_{c.s}-\Delta A \qquad (33)$$

The result of (33) is a reduction of the discrimination which the directional pattern of the antenna provides against an interferer. In Figs. 10 - 12, curves of (*C/I*) versus $\theta$ are presented for various locations (Japan, Florida and Denmark) as before and for realistic values of the above parameters in eq. (32). A list of these values is presented in Table 2. The numerical results taken from both predictive techniques (existing and modified) are given for various values of the percentage non-exceedance conditional probability ($p$%). A useful extract deduced from these diagrams is the estimation of a threshold for the angular separation between the satellites $\Theta_{th}$, less than this the operating system violates the specified interference tolerance conditions (e.g. for an allowed level of 28 dB for the (*C/I*) ratio and for the Florida area (Fig. 10),

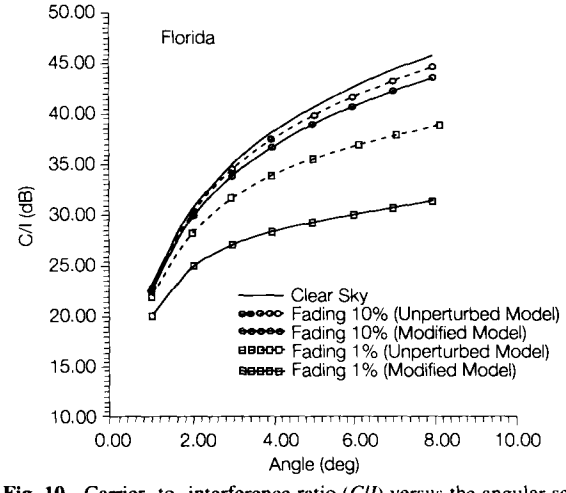


**Fig. 10** - Carrier -to- interference ratio (*C/I*) versus the angular separation ($\theta$), in comparison with the existing predictive results: $f$ = 15 GHz, $\varphi_1 = \varphi_2 = 30°$, $H_o$ = 0.2 km (Florida area, $\Lambda = 28°$).

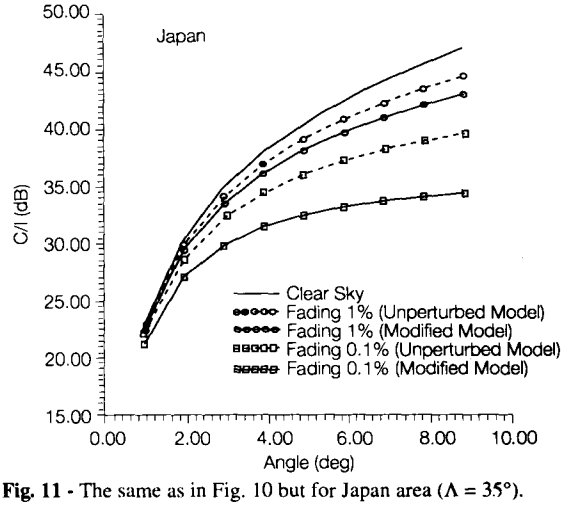


**Fig. 11** - The same as in Fig. 10 but for Japan area ($\Lambda = 35°$).

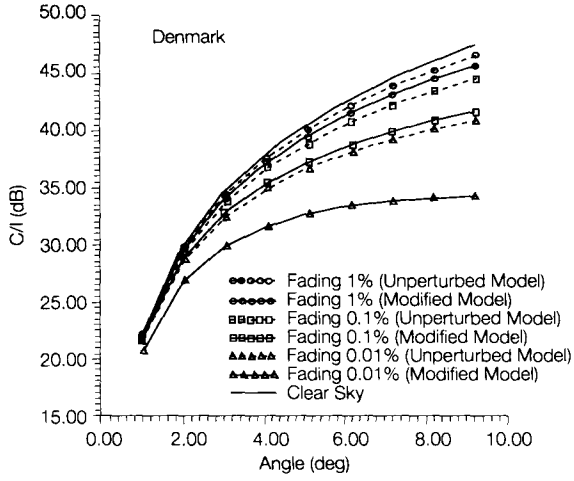


**Fig. 12** - The same as in Fig. 10 but for Denmark area ($\Lambda = 52°$).

the $\Theta_{th}$ can be found to be 1.6 (deg) for 10% and 2 (deg) for 1% non-exceedance conditional probability, respectively). As can be seen, the influence of the novel assumptions for the rain height, for all the cases, is more significant for the lower probabilities. Taking the previous example, the modified $\Theta_{th}$'s for 10% and 1% probabilities are 1.7 (deg) and 4 (deg) respectively. As a direct consequence, the demand for the design of earth-space

Table 2 - *Parameters of the (C/I) versus $\theta$ examples*

| Parameter | Value |
|---|---|
| $EIRP_s$ | 34 dBW |
| $EIRP_s'$ | 30 dBW |
| $G$ | 51 dB |
| $(C/I)_{nom}$ | $23 + 25 \log \theta$ |
| (A) Florida area | |
| $R_m$ | 0.0173 |
| $S_r$ | 2.45 |
| $G$ | 0.75 km |
| $M$ | 53 dB |
| (B) Japan area | |
| $R_m$ | 0.04964 |
| $S_r$ | 1.8677 |
| $G$ | 1.5 km |
| $M$ | 42 dB |
| (C) Denmark area | |
| $R_m$, $S_r$ | $F$ climatic zone |
| $G$ | 1.75 km |
| $M$ | 35 dB |

systems less interfered by other adjacent operating satellite links leads inevitably to the consideration of more accurate descriptions for the rain height.

As a final remark, we should note that motivation still exists for the further improvement of the analysis, by taking into account the anisotropic behaviour of the spatial rainfall correlation function which is quite significant for several locations around the world [18], or other models (except lognormal), such as a modified gamma form [19], for the representation of the point rainfall statistics.

## 4. Conclusions

Differential rain attenuation is considered to be one of the main propagation effects on interference between adjacent Earth-space paths. In this paper, a modification of an already existing systematic procedure for the prediction of the differential rain attenuation, is presented. The modified procedure takes into account a more complicated but realistic model for the description of the rain height. The results of the proposed procedure are compared with simulated data taken from Montreal. The comparison shows an improved situation in relation to the existing method. Moreover, the difference between the existing results and the deduced ones after use of the novel assumptions for the rain height, for various geographic latitudes and climatic zones, is also considered.

It is generally shown that the induced modification is quite significant for problems associated with locations of high absolute latitude even for dry climatic zones. On the other hand, independent of climatic zone and latitude of the location, the need for design of earth-space systems suffering least interference problems due to differential rain attenuation, leads to the inevitable use of more realistic considerations for the rain height.

*Manuscript received on May 30, 1995.*

## References


[1] R. R. Rogers, R. L. Olsen, J. L. Strickland, G. M. Coulson: *Statistics of differential rain attenuation on adjacent Earth-space propagation paths.* "Ann. Telecommun.", Vol. 37, No. 11-12, 1982, p. 445-452.

[2] CCIR: *Propagation data required for evaluating interference between stations in space and those on the surface of the Earth.* Report 885* (MOD I), Doc. 5 (1047-E), Int. Telecommunication Union, 1985, Geneva.

[3] J. D. Kanellopoulos, V. A. Houdzoumis: *A model for the prediction of differential rain attenuation on adjacent Earth-space propagation paths.* "Radio Sci.", Vol. 25, No. 5, 1990, p. 853-864.

[4] J. D. Kanellopoulos, S. Ventouras, C. N. Vazouras: *A revised model for the prediction of differential rain attenuation on adjacent Earth-space propagation paths.* "Radio Sci.", Vol. 28, No. 6, 1993, p. 1071-1086.

[5] J. D. Kanellopoulos, S. Ventouras, S. G. Koukoulas: *A model for the prediction of the differential rain attenuation between a satellite path and an adjacent terrestrial microwave system based on the two-dimensional gamma distribution.* "Jour. of Elec. Waves and Appl.", Vol. 8, No. 5, 1994, p. 557-574.

[6] J. D. Kanellopoulos, C. Sofras: *Predictive analysis of the differential rain attenuation between a satellite path and an adjacent terrestrial microwave system.* "Trans. on the IEICE of Japan", Vol. E76-B, No. 7, 1993, p. 768-776.

[7] R. K. Crane: *Prediction of attenuation by rain.* "IEEE Trans. Commun.", Vol. COM-28, 1980, p. 1717-1733.

[8] W. L. Stutzman, W. K. Dishman: *A simple model for the estimation of rain-induced attenuation along earth-space paths at millimeter wavelengths.* "Radio Sci.", Vol. 17, No. 6, 1982, p. 1465-1476.

[9] J. Goldhirsh, I. Katz: *Useful experimental results for earth-satellite rain attenuation modeling.* "IEEE Trans. Antennas Prop.", Vol. AP-27, No. 3, 1979, p. 413-415.

[10] J. D. Kanellopoulos, S. N. Livieratos: *A modified analysis for the prediction of multiple site diversity performance in Earth-space communication.* "Jour of Elec. Waves and Appl.", Vol. 11, 1997, p. 483-510.

[11] COST 210 Management Committee Commission of European Communities: *Influence of the atmosphere on interference between radio communications systems at frequencies above 1 GHz.* Cat. No CD-NA-13407-EN-C, ISBN 92-826-2400-5, 1991, Brussels.

[12] R. L. Olsen, D. V. Rogers, R. A. Hulays, M. M. Z. Kharadly: *Interference due to Hydrometeor Scatter on Satellite Communication Links.* "Proc. of the IEEE", Vol. 81, No. 6, 1993, p. 914-922.

[13] CCIR: *Radiometeorological data.* Report 563-2, Int. Telecommunication Union, 1982, Geneva.

[14] S. H. Lin: *A method for calculating rain attenuation distribution on microwave paths.* "Bell Syst. Tech. J.", Vol. 54, No. 6, 1975, p. 1051-1086.

[15] A. Papoulis: *Probability, Random Variables and Stochastic Processes.* Mc Graw-Hill, 1965, New York.

[16] R. R. Rogers, S. Radhakant, O. Massambani: *New radar studies of slant-path attenuation due to rain.* "Ann. Telecommun.", Vol. 36, No. 1-2, 1981, p. 40-47.

[17] T. T. Ha: *Digital satellite communications.* Mac Millan, 1986, New York.

[18] D. C. Hogg, T. S. Chu: *The role of rain in satellite communications.* "Proc. IEEE", Vol. 63, No. 9, 1975, p. 1308-1331.

[19] F. Moupfouma: *Model of rainfall-rate distribution for radio system design.* "Proc. Inst. Electr. Eng. Part H", Vol. 132, No. 1, 1985, p. 39-43.